Load dependence of two-dimensional atomic-scale friction

Satoru Fujisawa, Eigo Kishi, Yasuhiro Sugawara, and Seizo Morita
Department of Physics, Faculty of Science, Hiroshima University, 1-3-1 Kagamiyama, Higashi-Hiroshima, 739, Japan
(Received 3 April 1995)

We investigated the load dependence of two-dimensional atomic-scale friction between a MoS_2 surface and a Si_3N_4 tip. We found that the amplitude of the frictional force hysteresis is determined by the effective adhesive radius itself. Besides, we observed nearly zero kinetic frictional force at the normal load of 2.3×10^{-8} N. The load dependence of the effective adhesive radius suggests that the appearance of the negative frictional force correlates clearly with the load dependence.

The load dependence of the frictional force at the macroscopic scale is widely known as the Amontons-Coulomb law, where the frictional force is roughly proportional to the normal load. It is interpreted as an increase of the real contact area at multicontact asperities due to plastic deformation by the normal load. In order to study the mechanism of the friction in more detail, the load dependence of each contact asperity, i.e., single-asperity friction, should be investigated rather than the multicontact asperities. The load dependence of single-asperity friction on an atomic scale was investigated by Mate and co-workers, and they found that the frictional force is also roughly proportional to the normal load under a normal load of order 10^{-6} N.[1,2] Mayer *et al.* also studied the load dependence of single-asperity friction under a normal load between 2×10^{-9} and 1.6×10^{-8} N, and they concluded that there is no significant load dependence below 10 nN.[3]

Recently, we also studied single-asperity friction, which is two-dimensional atomic-scale friction or two-dimensionally discrete friction with lattice periodicity,[4–8] although its load dependence has not yet been investigated. In this paper, we report on the load dependence of two-dimensional atomic-scale friction between a MoS_2 surface and a Si_3N_4 tip of single asperity, which is measured with a two-dimensional frictional force microscope (2D-FFM) (Refs. 6 and 8) and studied by a two-dimensional stick-slip model with an effective adhesive radius.[8]

In the present experiment with the 2D-FFM, we measured the two-dimensional frictional force vector (f_X, f_Y) between the tip apex and the atomically flat surface with a raster scan at various normal loads between 2.3×10^{-8} and 4.7×10^{-7} N. Here we define X, Y, and Z directions as across, along, and normal to the cantilever, respectively.[4–8] We used a weak feedback control of the Z direction to the deflection signal in order to compensate for the slow Z-direction drift. As an atomically flat surface, we used a cleaved (0001) surface of MoS_2. Its lattice structure shows threefold symmetry with a lattice constant of 3.16 Å.[9] Soon after cleavage of the surface, measurements were performed in air under ambient conditions. As a cantilever, we used a rectangular microcantilever with a ~250-Å-curvature radius on a sharp tip apex which is made of Si_3N_4.[10] Its length, width, and thickness are 100, 40, and 0.8 μm, respectively. Its calculated nominal spring constants for Z and X directions are $k_Z=0.75$ N/m and $k_X=550$ N/m, respectively. The raster scan rate was set at ~400 Å/s for the fast line scan and ~0.80 Å/s for the slow scan. The area of the raster scan was 25×25 Å. For simplicity, we set both scan and X directions parallel to the [1000] direction of the MoS_2 surface.

Figures 1(a), 1(b), 1(c), and 1(d) show f_X data due to a fast line scan at the normal load of 2.3×10^{-8}, 5.3×10^{-8}, 1.2×10^{-7}, and 1.8×10^{-7} N, respectively. For simplicity, data at each normal load are those with the largest initial sticking among the 256 fast-line-scan data for different Y positions due to the slow scan. Line and dot data correspond to the fast-line scan from left to right and its reverse, which we call right and left scans for short, respectively. All f_Y data taken simultaneously with these f_X data of Fig. 1 show no fine structure within the noise, while all f_X data show sawtooth signals. Thus the estimated tip apex motion is a straight discrete jump with the lattice periodicity of MoS_2 surface[6,8] along the X

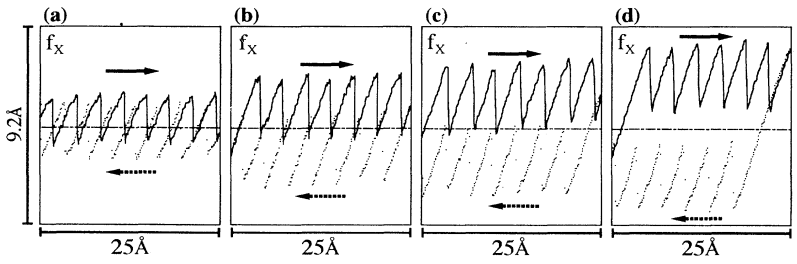

FIG. 1. (a), (b), (c), and (d) show fast-line-scan data of f_X at the normal load of 2.3×10^{-8}, 5.3×10^{-8}, 1.2×10^{-7}, and 1.8×10^{-7} N. The arrow indicates the scan direction. The dotted broken line shows the estimated zero level of f_X. Line and dot data correspond to the right and left scans, respectively.

0163-1829/95/52(7)/5302(4)/$06.00

direction, i.e., the scan direction. The scale of the vertical axis is calibrated by the lateral force curve,[7] and is the same for all data.

First we mention that we estimated the zero force level of f_X experimentally. Since the scan direction is just along the lattice structure and just across the cantilever, we can assume that there is no anisotropic factor between right and left scans. Thus the zero force level can be defined as the average of the signal due to the right and left scans, with which the observed data seem to agree. The dotted broken lines shown in Fig. 1 indicate the deduced zero force level.

In Figs. 1(a), 1(b), and 1(c), the sawtooth signals cross over the zero force level, which means the appearance of the negative frictional force[11,12] for both the right and left scans. This negative frictional force can be explained by a two-dimensional stick-slip model with an effective adhesive radius,[8] as shown in Fig. 2.

The effective adhesive radius (or distance) r is defined as the two-dimensional displacement of the cantilever required to overcome the sticking force f_{st} between the tip and stick point, i.e., f_{st}/k. When the scan point is within the area that r makes around the stick point, which is the effective adhesive area, the tip sticks to the stick point because the cantilever force cannot overcome f_{st}. On the other hand, when the scan point reaches the edge of the area, the tip slips. Here the scan point means the point of the tip apex with zero displacement for X or Y directions. By the fast-line scan, the trace of the scan point makes a line, namely, the scan line. The distance d between the stick point and scan line creates the force component of kd across the scan direction. This force component of kd works against the sticking force in addition to the ordinary frictional force component along the scan direction. To simplify the discussion, both f_{st} and the spring constant of the cantilever k are assumed to be constant and independent of directions. Thus r is defined as a constant value, which makes the effective adhesive area a round circle. Now we call r the effective adhesive radius, which is a radius of the effective adhesive area. When the displacement along the scan direction becomes $(r^2-d^2)^{1/2}$, the resultant cantilever force becomes equal to f_{st} and the tip apex slips. We call this place the slip place.

For simplicity, we concentrate on the case of two-dimensional stick-slip motion between only three stick points. The stick point is represented by the small closed circle. The effective adhesive area is represented by the large empty circle whose center is the stick point. The slip place is represented by the small empty circle at the cross point of the scan line and the edge of the effective adhesive area. The lattice periodicity of 3.16 Å and the effective adhesive radius are represented by l and r, respectively. We start the scan point from the left end of the scan line to the right. While the tip sticks to stick point A, by the scan the scan point travels along the scan line in the effective adhesive area A with increasing f_X. When the scan point arrives at the edge of the effective adhesive area A, i.e., the slip place 1, the resultant cantilever force at $f_X=k_X\sqrt{r^2-d^2}$ and $f_Y=k_Y d$ becomes equal to the sticking force, and the tip slips out of this effective adhesive area. Now the tip slips straightly along the direction from stick point A to slip place 1 due to the cantilever force and does not reach the next stick point B for $d\neq 0$, if there exists no force that attracts the tip apex toward the next stick point B. The experimentally observed signals, however, suggest that the tip takes a straight walk along the X direction even for $d\neq 0$,[6] which means that the tip slips or jumps from stick points A to B.[8] This confirms that the tip is attracted by the next stick point B. We assume that this attractive force affects the tip since slip place 1 is in the effective area B shown in Fig. 2, and that the effective adhesive area is the kind of field that attracts the tip apex during the slip motion. When the effective adhesive radius r is smaller than the lattice constant l, as shown in Fig. 2, slip place 1 is between stick points A and B with respect to the X direction. Thus the direction of the X component of the attractive force is reversed between just before and just

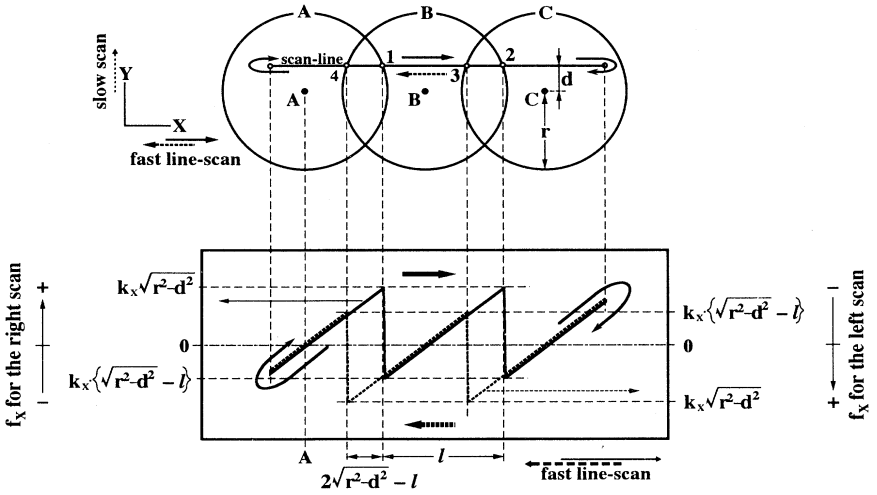

FIG. 2. Two-dimensional stick-slip model with effective adhesive radius for one fast line-scan shows the definition of hysteresis of f_X between the right and left scans. The tip apex sticks to and slips between stick points A, B, and C. Note that the direction, i.e., the sign of the f_X, is reversed between the lined and dotted sawtooth signals due to the right and left scans, respectively.

after the slip. This confirms to us that the f_X value of $k_X\sqrt{r^2-d^2}$ just before the slip is positive, and that the f_X of $k_X\{\sqrt{r^2-d^2}-l\}$ just after the slip, i.e., at the beginning of the stick, is negative. On the other hand, when r becomes larger than l, slip place 1 appears at the right of stick point B at least for $d=0$. Thus the direction of the X component of the attractive force is always positive, i.e., $k_X\{\sqrt{r^2-d^2}-l\}$ is positive for $r>l$ at least $d=0$. This corresponds to the data shown in Fig. 1(d).

As shown in Fig. 2, while the tip is sticking to stick point B, the cantilever force also increases by the scan. Just after the scan point reaches slip place 2, the tip slips to stick point C. This is the same as the stick-slip process from stick points A to B. Thus by increasing the number of stick points in a fast-line scan, the number of the same stick-slip process simply increases. At the right end of the scan line the scan direction is reversed, so that the direction of the frictional force, i.e., the sign of f_X or the vertical axis, is also reversed, as shown in Fig. 2. For the left scan, the frictional force values are also $k_X\sqrt{r^2-d^2}$ just before slip and $k_X\{\sqrt{r^2-d^2}-l\}$ just after the slip. Thus the stick-slip process for the left scan is the same as that for the right scan except that the sign of f_X is reversed, as shown in Fig. 2. At the left end of the scan line, this fast-line-scan loop is completed. Then the scan direction is again reversed and the next fast-line scan begins after the slow scan. As a result we can see the hysteresis formed by the right and left scans, which consists of lateral and vertical shifts between the sawtooth signals for the right and left scans. Both shifts are due to the difference of the slip places between the right and left scans, for instance the difference between slip places 1 and 4, or 2 and 3. As a result, the lateral and vertical shifts are represented by the scan distance between these slip places as $2\sqrt{r^2-d^2}-l$ and the resulting frictional force difference of $k_X\{2\sqrt{r^2-d^2}-l\}$, respectively. Thus r determines the amplitude of the hysteresis, since l is constant and d changes only periodically with 2.74 Å by the slow scan.

In order to investigate experimentally the dependence of r on the normal load, we estimated the amplitude $\sqrt{r^2-d^2}$ of the hysteresis from the experimental results at each normal load. The closed circles in Fig. 3 show the value of $d=0$, i.e., the maximum value of $\sqrt{r^2-d^2}$, where part of the data is estimated from Fig. 1. Thus the closed circle shows the normal load dependence of r itself. The bars in Fig. 3 show the change of $\sqrt{r^2-d^2}$, which is due to the change of d by the slow scan. As shown in Fig. 3 the experimental value of the effective adhesive radius r increases by increasing the normal load. Above the normal load of 1.8×10^{-7} N, r increases roughly proportionally to the normal load as indicated by the broken line. On the other hand, below 1.2×10^{-7} N the data deviate from the broken line, and the load dependence becomes weaker. In addition, the negative frictional force appears below 1.2×10^{-7} N, as shown in Fig. 1(c). This coincidence seems to suggest that the appearance of the negative frictional force correlates clearly with the normal load dependence of the effective adhesive radius.

In order to relate the atomic-scale friction described above with static and kinetic frictions of the macroscopic friction concept, we consider the energy transfer in the straight stick-slip process with the periodicity l. During one stick period the cantilever spring stores the elastic energy, which is expressed as

$$\int_0^l \mathbf{f}\,d\mathbf{s}=\int_0^l (f_X,f_Y)(ds_X,ds_Y=0)$$
$$=\int_0^l f_X\,ds_X=k_X\int_0^l s_X\,ds_X\ . \tag{1}$$

Here the scan direction is also defined as the X direction, so that the subscript X means the component along the scan direction. $\mathbf{f}=(f_X,f_Y)$ is the frictional force, k_X is the spring constant of the cantilever along the scan direction, and s_X is the scan distance of the scan point during the stick. This energy is released by the slip motion of the tip. When this slip motion is treated as the macroscopic friction, this energy is consumed by the kinetic frictional force f_k during the slip motion. This is expressed as

$$\int_0^l f_k\,ds_X=f_k l\ . \tag{2}$$

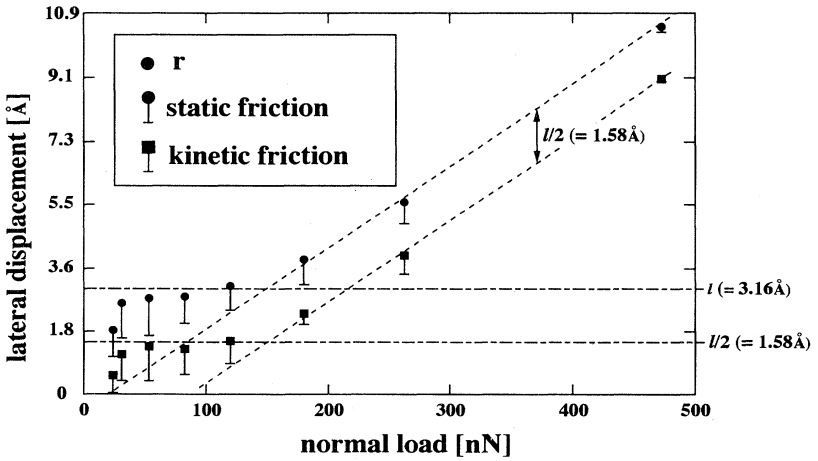

FIG. 3. Under the macroscopic definition of the frictional force, the experimentally estimated displacement due to the static frictional force of $\sqrt{r^2-d^2}$ and the displacement due to the kinetic frictional force of $\sqrt{r^2-d^2}-l/2$ at each normal load are plotted by the closed circle and the empty square with bars, respectively. The closed circles and empty squares correspond to the data for $d=0$. The bars are due to a change of d by the slow scan. The closed circles correspond to the effective adhesive radius r itself.

From Eqs. (1) and (2),

$$\frac{f_k}{k_X}=\frac{1}{l}\int_0^l s_X ds_X \tag{3}$$

are obtained. By using Eq. (3), the kinetic frictional force f_k in the straight stick-slip motion with the lattice periodicity of l, i.e., the case of Fig. 2, is expressed as

$$\frac{f_k}{k_X}=\sqrt{r^2-d^2}-\frac{l}{2}\ . \tag{4}$$

On the other hand, the static friction under the macroscopic definition is given by $k_X\sqrt{r^2-d^2}$, which is the frictional force just before the slip. Thus the difference between the static and kinetic frictional forces should be

$$k_X\sqrt{r^2-d^2}-k_X\{\sqrt{r^2-d^2}-l/2\}=k_X l/2\ . \tag{5}$$

This value is due to the discreteness of the stick-point distribution with the periodicity of l.

According to Eq. (4) the experimentally estimated f_k/k_X for $d=0$ is deduced by subtracting half the amplitude of the sawtooth signal from the experimentally estimated static friction at each normal load, and is plotted as the closed empty square in Fig. 3. The bar shows the change of f_k due to the change of d by the slow scan. From Eq. (4) one can see that, as $\sqrt{r^2-d^2}$ becomes close to $l/2$, f_k becomes close to zero. At that time, the hysteresis of $2\sqrt{r^2-d^2}-l$ disappears, which means the disappearance of the shift of the slip places between the right and left scans in Fig. 2. The data shown in Fig. 3 show that, at the normal load of 2.3×10^{-8} N, f_k becomes close to zero. Thus the negative frictional force and the change of the load dependence seem to be a foreboding phenomena of nearly zero kinetic frictional force, although the change of the load dependence seems to keep the kinetic frictional force off zero.

The treatment described above is consistent only for straight stick-slip motion. This is because Eq. (2) of the macroscopic treatment does not include the intrinsic Y component across the scan direction. For example, the static frictional force is $k_X\sqrt{r^2-d^2}$ under the macroscopic definition, where the frictional forces are assumed to act only along the scan direction. The frictional force component across the scan direction of $k_Y d$, however, also acts against the sticking force, i.e., the attractive force from the stick point. Thus the static frictional force should be the resultant force of $k_X\sqrt{r^2-d^2}$ and $k_Y d$, i.e., the sticking force itself. Thus, for the atomic-scale friction, the frictional force should also be treated as a two-dimensional vector $\mathbf{f}$. Especially for the zigzag stick-slip motion,[4–8] a two-dimensional treatment of the frictional force seems to be essential.

We found that the effective adhesive radius defined by f_{st}/k depends on the normal load. However, the spring constant k does not depend on the normal load. As a result, f_{st} should depend on the normal load. This means that the interfacial interaction[13] between the MoS_2 atomically flat surface and tip depends on the normal load.

To conclude, we investigated experimentally the normal load dependence of two-dimensionally discrete friction with lattice periodicity between the MoS_2 surface and Si_3N_4 tip, and studied the result using the two-dimensional stick-slip model with an effective adhesive radius. Below the normal load of 1.2×10^{-7} N, we observed negative frictional force with an experimentally estimated zero frictional force level. We found that the two-dimensional stick-slip model with an effective adhesive radius can explain the negative frictional force. We also found that the amplitude of the frictional force hysteresis is determined by the effective adhesive radius itself, and that the load dependence of the effective adhesive radius suggests that the appearance of the negative frictional force correlates clearly with the load dependence. In addition, we observed nearly zero kinetic frictional force at the normal load of 2.3×10^{-8} N.

We thank Dr. T. Okada, S. Mishima, and S. Ito of Olympus Optical Co., Ltd. for the construction of the AFM/LFM unit. We also thank A. Toda and K. Matuyama of Olympus Optical Co., Ltd. for supplying the Si_3N_4 microcantilevers.

[1]C. M. Mate, G. M. McClelland, R. Erlandsson, and S. Chiang, Phys. Rev. Lett. **59**, 1942 (1987).

[2]R. Erlandsson, G. Hadziioannou, C. M. Mate, G. M. McClelland, and S. Chiang, J. Chem. Phys. **89**, 5190 (1988).

[3]E. Meyer, R. Overney, D. Brodbeck, L. Howald, R. Lüthi, J. Frommer, and H.-J. Güntherodt, Phys. Rev. Lett. **69**, 1777 (1992).

[4]S. Fujisawa, Y. Sugawara, S. Ito, S. Mishima, T. Okada, and S. Morita, Nanotechnology **4**, 138 (1993).

[5]S. Fujisawa, Y. Sugawara, S. Morita, S. Ito, S. Mishima, and T. Okada, J. Vac. Sci. Technol. B **12**, 1635 (1994).

[6]S. Fujisawa, E. Kishi, Y. Sugawara, and S. Morita, Jpn. J. Appl. Phys. **33**, 3752 (1994).

[7]S. Fujisawa, E. Kishi, Y. Sugawara, and S. Morita, Appl. Phys. Lett. **66**, 526 (1995).

[8]S. Fujisawa, E. Kishi, Y. Sugawara, and S. Morita, Phys. Rev. B **51**, 7849 (1995).

[9]J. A. Wilson and A. D. Yoffe, Adv. Phys. **18**, 193 (1969).

[10]Olympus Optical Co., Ltd., 2951 Ishikawacho Hachioji, 192 Japan.

[11]G. J. Germann, S. R. Cohen, G. Neubauer, G. M. McClelland, and H. Seki, J. Appl. Phys. **73**, 163 (1993).

[12]R. M. Overney, H. Takano, M. Fujihira, W. Paulus, and H. Ringsdorf, Phys. Rev. Lett. **72**, 3546 (1994).

[13]G. M. McClelland, *Adhesion and Friction,* Springer Series in Surface Sciences Vol. 17 (Springer-Verlag, Berlin, 1990), p. 1.